

## Formate-Induced Inhibition of the Water-Oxidizing Complex of Photosystem II Studied by EPR<sup>†</sup>

Yashar M. Feyziev,<sup>‡,§</sup> Daiki Yoneda,<sup>||</sup> Takahiko Yoshii,<sup>||</sup> Nobuhiro Katsuta,<sup>||</sup> Asako Kawamori,<sup>\*,||</sup> and Yasutaka Watanabe<sup>||</sup>

*Institute of Botany, Academy of Sciences, Patamdar shosse 40, Baku 370073, Azerbaijan, and Faculty of Science, Kwansei Gakuin University, 1-1-155 Uegahara, Nishinomiya, Hyogo 662-8501, Japan*

*Received October 25, 1999; Revised Manuscript Received December 27, 1999*

**ABSTRACT:** The effects of various formate concentrations on both the donor and the acceptor sides in oxygen-evolving PS II membranes (BBY particles) were examined. EPR, oxygen evolution and variable chlorophyll fluorescence have been observed. It was found that formate inhibits the formation of the S<sub>2</sub> state multiline signal concomitant with stimulation of the Q<sub>A</sub><sup>-</sup>Fe<sup>2+</sup> signal at  $g = 1.82$ . The decrease and the increase in intensities of the multiline and Q<sub>A</sub><sup>-</sup>Fe<sup>2+</sup> signals, respectively, had a linear relation for formate concentrations between 5 and 500 mM. The  $g = 4.1$  signal formation measured in the absence of methanol was not inhibited by formate up to 250 mM in the buffer. In the presence of 3% methanol the  $g = 4.1$  signal evolved as formate concentration increased. The evolved signal could be ascribed to the inhibited centers. Oxygen evolution measured in the presence of an electron acceptor, phenyl-*p*-benzoquinone, was also inhibited by formate proportionally to the decrease in the multiline signal intensity. The inhibition seemed to be due to a retarded electron transfer from the water-oxidizing complex to Y<sub>Z</sub><sup>+</sup>, which was observed in the decay kinetics of the Y<sub>Z</sub><sup>+</sup> signal induced by illumination above 250 K. These results show that formate induces inhibition of water oxidation reactions as well as electron transfer on the PS II acceptor side. The inhibition effects of formate in PS II were found to be reversible, indicating no destructive effect on the reaction center induced by formate.

Photosystem II (PS II)<sup>1</sup> in plants and cyanobacteria catalyzes the water oxidation and the reduction of plastoquinone, which are driven by absorbed light energy. Their reaction center (RC) consists of 32–34 kDa polypeptides, D<sub>1</sub> and D<sub>2</sub>, which contain the primary electron donor P<sub>680</sub> (dimer of chlorophyll *a*), the secondary electron donors Y<sub>Z</sub> and Y<sub>D</sub> (tyrosines), the intermediary electron acceptor pheophytin (Pheo), and two plastoquinone electron acceptors, Q<sub>A</sub> and Q<sub>B</sub>, along with an associated non-heme iron. Light absorption produces a charge-separated state, P<sub>680</sub><sup>+</sup>Pheo<sup>-</sup>, which is rapidly stabilized by the reduction of P<sub>680</sub><sup>+</sup> through oxidation of Y<sub>Z</sub> and by the oxidation of Pheo<sup>-</sup> through reduction of Q<sub>A</sub>, respectively. Oxidized tyrosine Y<sub>Z</sub><sup>+</sup> is

reduced by an electron transferred from the water-oxidizing complex. This complex includes a tetranuclear manganese cluster that is closely associated with the RC and stabilized by three extrinsic polypeptides (33, 24, and 18 kDa) as well as calcium and chloride ions. It has been accepted that the manganese ions in different oxidation states accumulate four oxidizing equivalents required for oxidation of water through five successive intermediate states, as denoted by S<sub>0</sub>, S<sub>1</sub>, ..., S<sub>4</sub> (1, 2).

Normal functions of PS II require bicarbonate (HCO<sub>3</sub><sup>-</sup>) (reviewed in refs 3–5). It has been shown that removal of bicarbonate from PS II membranes either by bubbling with CO<sub>2</sub>-free air (6, 7) or by the addition of formate (HCO<sub>2</sub><sup>-</sup>) (8–10), or nitric oxide (11, 12), etc. resulted in inhibition of light-induced electron transport in PS II. The inhibition of PS II, induced by bicarbonate depletion, is restored by the addition of bicarbonate (6, 7). At least two binding sites of bicarbonate in PS II were suggested in earlier previous studies, namely, (1) a high-affinity pool at a concentration of approximately one HCO<sub>3</sub><sup>-</sup> molecule per 300–400 molecules of chlorophyll and (2) a low-affinity pool at a concentration larger than that of the bulk chlorophyll (8). Shortly later the non-heme iron of the Q<sub>A</sub><sup>-</sup>Fe<sup>2+</sup> complex has been suggested to be the high-affinity site for bicarbonate and critical for controlling PS II activity (9). As one of the effects of formate on PS II, it has been shown that formate competes with bicarbonate for the binding to the non-heme iron at the acceptor side of PS II and slows the electron transfer from Q<sub>A</sub><sup>-</sup> to Q<sub>B</sub> (11–15).

<sup>†</sup> This work was partly supported by the Hyogo Science and Technology Association. Y.M.F. is indebted to Kwansei Gakuin University for a postdoctoral fellowship for his work there.

\* To whom correspondence should be addressed. Phone: 81-798-54-6393. Fax: 81-798-51-0914. E-mail: kawamori@kwansei.ac.jp.

<sup>‡</sup> Academy of Sciences.

<sup>§</sup> Present address: Department of Biochemistry, Centre for Chemistry and Chemical Engineering, Lund University, P.O. Box 124, S-22 100 Lund, Sweden.

<sup>||</sup> Kwansei Gakuin University.

<sup>1</sup> Abbreviations: PS II, photosystem II; RC, reaction center; Chl, chlorophyll; WOC, water-oxidizing complex; P<sub>680</sub>, primary electron donor of PS II; Pheo, intermediary acceptor pheophytin of PS II; Q<sub>A</sub>, the primary electron acceptor quinone of PS II; Q<sub>B</sub>, the secondary acceptor quinone of PS II; Y<sub>Z</sub>, tyrosine-161 of the D<sub>1</sub> polypeptide; Y<sub>D</sub>, tyrosine-161 of the D<sub>2</sub> polypeptide; PPBQ, phenyl-*p*-benzoquinone; MES, 2-(*N*-morpholino)ethanesulfonic acid; EDTA, ethylenediamine-tetraacetic acid; DCMU, 3-(3,4-dichlorophenyl)-1,1-dimethylurea. ESE, electron spin-echo.

The requirement of bicarbonate for the function of the PS II donor side has been suggested recently (16–20). The reversibility of the formate/bicarbonate effects on light-induced electron transport (16, 17) and the changes in the absorption of Mn at the UV region were demonstrated for the oxygen-evolving PS II membranes (18). The function of bicarbonate was described as facilitating the binding of  $\text{Mn}^{2+}$  to the reaction center since bicarbonate stimulated rebinding of exogenous  $\text{Mn}^{2+}$  to the Mn-depleted PS II preparations (19). These experiments suggested that the donor side of PS II is also a high-affinity site for binding of bicarbonate.

In this study we used sodium formate to remove bicarbonate from the binding sites. The EPR signals of the  $\text{S}_2$  state manganese cluster and  $\text{Q}_\text{A}^-\text{Fe}^{2+}$  complex, variable fluorescence of chlorophyll, and oxygen-evolving activity were measured in PS II membranes treated with formate. We found that the inhibition in the multiline signal formation and the oxygen evolution are correlated with the formate-induced  $\text{Q}_\text{A}^-\text{Fe}^{2+}$  signal observed at the  $g = 1.82$  magnetic field position. The results presented here suggest that formate may also contribute to inhibition in water oxidation reactions on the donor side as well as in electron transfer on the acceptor side of PS II.

## MATERIALS AND METHODS

**Sample Preparations.** PS II enriched membrane fragments (BBY particles) were prepared from market spinach using a method as described in ref 21 with modifications (22). All steps of preparations were performed under dim green light. BBY particles at a chlorophyll concentration of 10 mg/mL, determined according to Arnon (23), were suspended in solution A [50 mM MES–NaOH (pH 6.0) and 35 mM NaCl] and stored at 77 K with 50% glycerol added until use. Prior to the experiment, the membranes were thawed slowly at 2 °C and washed twice with solution B [50 mM MES–NaOH (pH 6.0), 5 mM NaCl, 5 mM  $\text{CaCl}_2$ , 300 mM sucrose, and 1 mM EDTA] by centrifugation at 30000g for 20 min. In some experiments another method of preparation (KM particles (24)) was applied.

Sodium formate treated PS II membranes were prepared as described for acetate treatment in ref 25. The PS II membranes were washed twice with solution B with supplemental addition of sodium formate at varying concentrations between 25  $\mu\text{M}$  and 500 mM by centrifugation at 30000g for 20 min. Before the last centrifugation, 3% methanol was added to quantify the multiline signal intensity. This treatment was performed according to ref 26 by incubating PS II membranes at a chlorophyll concentration of 0.3 mg/mL in 0.8 M Tris–HCl (pH 8.4) for 30 min under room light at 2 °C followed by centrifugation and resuspending in buffer A.

For EPR measurements the final pellet at chlorophyll concentrations 20–25 mg/mL, which is concentrated at about 5 times the final concentration, was collected and transferred into Suprasil quartz tubes of 4 mm inner diameter. The samples were incubated under the dark in ice–water for 60 min to equilibrate PS II in a dark stable  $\text{S}_1$  state, and then stored in liquid nitrogen until EPR measurements. To observe the multiline signal in the  $\text{S}_2$  state of PS II, the sample was illuminated by a 500 W tungsten bromide lamp at 200 K

for 10 min, and then frozen rapidly in liquid nitrogen. The  $\text{Y}_\text{Z}^+$  radical was trapped by illumination at 253 K for 1 min and immediate freezing of the sample in liquid nitrogen as described in refs 26 and 27.

For measurement of chlorophyll fluorescence and  $\text{O}_2$  evolution, the pellet of formate-treated samples was resuspended in a small volume of solution A to give a final chlorophyll concentration of 3 mg/mL, and the homogenate was stored on ice. Before measurement of fluorescence intensity and  $\text{O}_2$  evolution, 10  $\mu\text{L}$  of the homogenate was added to 3 mL of the assay medium with varying formate concentrations to give a final chlorophyll concentration of 10  $\mu\text{g/mL}$ . All procedures of formate treatment were performed under dim green light.

**Oxygen Evolution.** The oxygen-evolving activity was measured using a Clark-type electrode at 25 °C under continuous illumination at the saturating intensity through a  $\lambda > 650$  nm Toshiba R50 glass filter and 5 cm thick water filter. In the presence of 100  $\mu\text{M}$  PPBQ as an electron acceptor, the rate of oxygen evolution of the control samples was  $400 \pm 20 \mu\text{mol of O}_2 (\text{mg of Chl})^{-1} \text{h}^{-1}$ .

**Fluorescence Measurements.** The photoinduced changes of chlorophyll fluorescence yield  $F_\text{V}$  were measured at 25 °C using a home-built spectrometer at a chlorophyll concentration of 10  $\mu\text{g/mL}$ . In this spectrometer  $\lambda = 490$  nm weak (0.05  $\text{W/m}^2$ ) measuring light was used for fluorescence excitation, while  $\lambda > 650$  nm (50 or 150  $\text{W/m}^2$ ) actinic light was used to induce photochemical reaction in reaction centers.

**EPR Experiments.** EPR measurements were performed using a Bruker-300E X-band spectrometer, and an ST4102 standard cavity. An Oxford-900 continuous gas flow cryostat and ITC-4 temperature controller were used to regulate the sample temperature at 6.0 K. To avoid saturation, the multiline signal was observed at a microwave power of 3.2 mW. The  $\text{Y}_\text{Z}^+$  signal was observed at 77 K, using a finger-type liquid nitrogen dewar. After measurement of  $\text{Y}_\text{D}^+$  and  $\text{Y}_\text{Z}^+$  signals in the sample trapped after illumination, the sample was dark adapted at 0 °C for 30 min. The resulting signal of  $\text{Y}_\text{D}^+$  was used as a background signal to obtain the net  $\text{Y}_\text{Z}^+$  signal. To identify the  $\text{Y}_\text{Z}^+$  and  $\text{Y}_\text{D}^+$  radical pair in the trapped sample, the “2 + 1” pulse sequence ESE method was applied using a Bruker 380 pulse accessory and a dielectric cavity as described in ref 26. For quantification of the  $\text{S}_2$  state signals, the multiline and  $g = 4.1$  signal intensities were estimated for control PS II with and without methanol addition on the basis of the  $\text{Y}_\text{D}^+$  radical signal intensity observed at 6 K.

## RESULTS

**$\text{S}_2$  State Multiline Signal.** Illumination of the oxygen-evolving PS II preparations at 200 K results in formation of the dark stable  $\text{S}_2$  state of PS II. The  $\text{S}_2$  state EPR spectra obtained for various concentrations of formate at pH 6.0 are shown in Figure 1. This state is characterized by two kinds of EPR signals: the  $g = 1.98$  signal, denoted as the multiline, and the  $g = 4.1$  signal (28–33). The spectra consist of at least 18 well-resolved lines (Figure 1a,e) ascribed to the  $S = 1/2$  ground spin state of an antiferromagnetically exchange-coupled Mn tetramer, as described in refs 33–35. In addition, the control sample without methanol produced the  $g = 4.1$

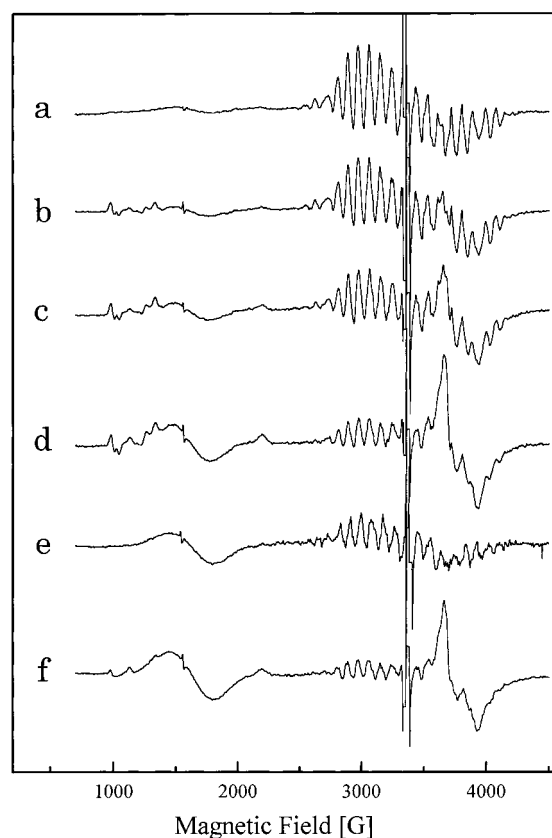


FIGURE 1: EPR spectra of untreated (a) and 10 mM (b), 100 mM (c), and 250 mM (d) formate treated BBY PS II samples in the presence of 3% methanol and the control PS II without methanol addition (e) and in the presence of 250 mM formate (f) at pH 6.0. All spectra have been normalized by a  $Y_D^+$  radical signal observed at a microwave power of  $0.8 \mu\text{W}$  and field modulation amplitude of 3.2 G. The difference (200 K illuminated – dark) spectra were obtained with PS II membranes at pH 6.0 in the buffer of 50 mM MES–NaOH, 300 mM sucrose, 5 mM NaCl, 5 mM  $\text{CaCl}_2$ , and 1 mM EDTA. Experimental conditions: microwave frequency 9.42 GHz, microwave power 3.2 mW, modulation amplitude 10 G, temperature 6 K. Each of the spectra is a result of two scans of field sweep.

signal (Figure 1e) ascribed to an  $S = 3/2$  or  $5/2$  spin state of the Mn cluster (30, 32–34, 36, 37). The addition of 3% methanol to the control PS II inhibited the  $g = 4.1$  signal formation from the Mn cluster upon illumination (Figure 1a). Treatment of the membranes with formate of up to 10 mM gave no remarkable effect on the spectrum (Figure 1b). This result is contradictory to the previous suggestions (16, 17) that the inhibitory effect of low concentrations of formate on the donor side reactions was found by the measurement of variable fluorescence of chlorophyll. Inhibition of formation of the Mn multiline signal occurred in the samples treated with high concentrations ( $>10$  mM) of formate, as shown in the spectra at 100 and 250 mM formate (Figure 1c,d), respectively. The inhibition occurred rather drastically at formate concentrations between 10 and 100 mM and gradually saturated at above 100 mM formate. In samples treated with 250 and 500 mM formate, the similar intensity of the remaining multiline signal of  $25 \pm 15\%$  of that in a control sample was observed. No changes in the hyperfine splitting in the multiline signal for formate-treated membranes were observed, indicating that the remaining signal can be assigned to noninhibited sites.

Table 1: Intensity Relation between the Multiline and  $g = 4.1$  Signals Divided by the  $Y_D^+$  Signal Intensity<sup>a</sup>

sample	integrated intensity		
	multiline	$g = 4.1$	sum
PS II with 3% methanol	0.96	0.04	1.0
PS II without methanol	0.53	0.47	1.0
methanol + 250 mM formate	0.34	0.87	1.21
250 mM formate	0.29	1.30	1.59

<sup>a</sup> The errors in calculation were about  $\pm 0.1$  for the multiline signals and 0.04 for the  $g = 4.1$  signals, respectively.

The  $g = 4.1$  signal gradually developed (Figure 1b–d) with increasing formate concentrations at 10–250 mM. Above 100 mM formate concentration an appreciable  $g = 4.1$  signal intensity was observed even in the presence of 3% methanol (Figure 1d). The intensity was comparable to that in a control sample without methanol as shown in Figure 1e. With an increase in formate concentration up to 250 mM, the  $g = 4.1$  signal intensity increased whereas the multiline signal intensity decreased. However, the  $g = 4.1$  signal intensities decreased above 250 mM formate. The sharp signals around the  $g = 5$ –6 region in Figure 1d,f can be ascribed to some photooxidized  $\text{Fe}^{3+}$ , which might be due to heme or non-heme iron in some nonnative sites of PS II (38), and whose intensity could be negligible. The small signals at about  $g = 3$  in the same traces are assigned to a minor quantity of photooxidized cyt b559 in which some structural changes might have occurred during preparation. These signals were not observed in the other method of preparation of PS II membranes (24), though most of the experimental data indicate similar characteristics (data not shown).

The inhibitory effect of high concentrations of formate on the multiline signal intensity could be eliminated by washing the formate-treated membranes with the formate-depleted buffer. The addition of bicarbonate (5–10 mM) during 25 mM formate treatment similarly prevented the inhibition. In some control samples treated with 5–10 mM bicarbonate, a slight increase in the multiline signal intensity was observed. Because of alkalization of the assay medium at high concentrations of bicarbonate, the bicarbonate effect on the multiline signal intensity in the formate-inhibited PS II particles could not be determined in further detail.

We have compared the multiline signal intensity of the control PS II samples with and without methanol addition. In the PS II sample without methanol (Figure 1e) the multiline signal intensity estimated by the peak-to-peak height was about half that with methanol (Figure 1a). This decrease can be considered to correlate with the increase in the  $g = 4.1$  signal intensity, since the addition of methanol up to 5% did not inhibit oxygen-evolving activity. However, a small difference was found in the line width and the shape of the multiline signals in PS II samples with and without methanol. We have estimated the intensities of both signals by double integration and have shown the values divided by the  $Y_D^+$  signal intensity in each sample in Table 1. In PS II with 3% methanol, the multiline signal intensity was estimated to be 96% and the weak  $g = 4.1$  signal intensity to be 4% on the basis of the  $Y_D^+$  signal intensity. From the values of both samples the decrease in the multiline signal intensity was estimated to be about 43% for PS II without



Table 2: Intensity of Formate-Induced  $Q_A^-Fe^{2+}$  Signals in PS II with 500 mM Formate Concentration<sup>a</sup>

PS II with methanol	PS II without methanol	Tris-treated PS II
0.66	0.50	0.97

<sup>a</sup> The values are given by division by the  $Y_D^+$  signal intensity. The error in estimation is about  $\pm 0.1$ .

methanol. Therefore, the intensity of the  $g = 4.1$  signal can be considered to correspond to 47% of the  $S_2$  state. If we assume the  $g = 4.1$  signal to be ascribed to the active  $S_2$  state in the formate-treated PS II, the quantitation shows that the summation of the multiline and  $g = 4.1$  signal intensities reaches values of almost 120% and 160% at 250 mM formate with and without methanol, respectively. These values should decrease with increasing formate concentration. Therefore, we have to consider the formate-induced  $g = 4.1$  signal to be ascribed to an inactive site. In PS II with 3% methanol we took the multiline signal site only into consideration as the active center. We could not estimate the active  $S_2$  state in the control sample without methanol, because the formate-treated sample included both active and inactive  $g = 4.1$  signal sites that could not be separated. The formate-induced  $g = 4.1$  signal may be ascribed to a different spin state of the Mn cluster with a modified structure, though the line shape was quite similar to that for the active  $g = 4.1$  signal.

**$Q_A^-Fe^{2+}$  Signal.** It has been reported that binding of formate stimulated the EPR signal at  $g = 1.82$  due to the photoinduced  $Q_A^-Fe^{2+}$  state of the PS II acceptor complex (39). In this experiment, the signal due to the  $Q_A^-Fe^{2+}$  acceptor complex in the  $g < 2.0$  region was not observed at the low microwave power of 3.2 mW in a control PS II sample. This signal developed in formate-treated samples illuminated at 200 K for concentrations of more than 10 mM and was accompanied by a decrease in the Mn multiline signal intensity as seen in Figure 1b–d,f. The signal increased as the formate concentration increased and seemed to be saturated at formate concentrations over 250 mM. The signal disappeared after depletion of formate from the treated membranes.

The quantitation of the  $Q_A^-Fe^{2+}$  signal intensity was carried out on the Tris-treated PS II with 500 mM formate concentration to determine the ratio of the formate-induced signal in formate-treated samples. The  $Q_A^-Fe^{2+}$  to  $Y_D^+$  signal intensity ratios are shown in Table 2. On the basis of value of 97% for Tris-treated PS II with 500 mM formate, the dependencies of the decrease in the multiline and evolution of the  $Q_A^-Fe^{2+}$  signal intensities on formate concentration are shown in Figure 2A, indicating a stoichiometric proportionality between their dependencies as drawn in a different way in Figure 2B.

**$Y_Z^+$  Signal.** Figure 3A shows the appearance of the  $Y_Z^+$  signal observed at 77 K in the KM particles in the presence of 250 mM formate trapped after illumination at 253 K. Trace 1 shows the  $Y_D^+$  signal observed in the dark-adapted sample. Trace 2 shows the  $Y_D^+$  and  $Y_Z^+$  in the trapped sample after illumination, in which the signal intensities increased as compared to those of the trace 1. This is in contrast with that obtained for untreated PS II membranes. The subtracted signal in trace 3 can be ascribed to the  $Y_Z^+$  signal that gives evidence that electron donation from WOC to  $Y_Z^+$  became slower in the presence of formate. The intensity of the

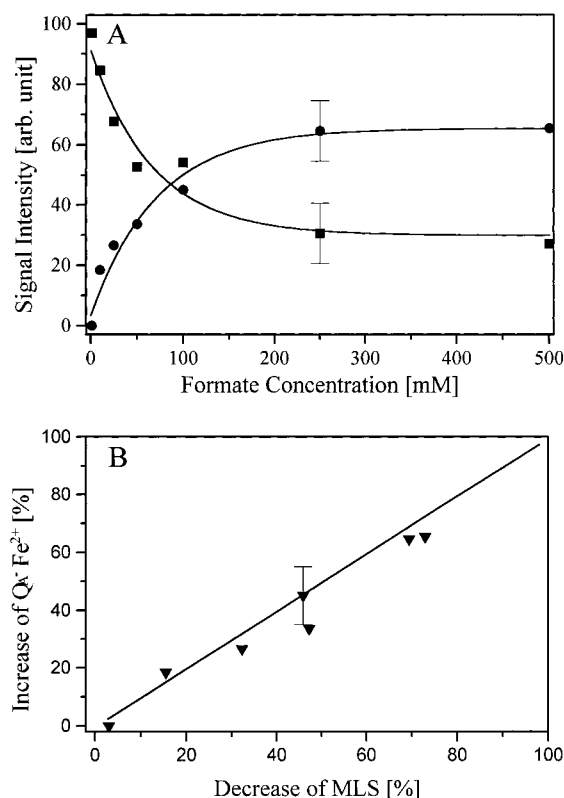


FIGURE 2: (a) Dependence of  $S_2$  state multiline (squares) and  $Q_A^-Fe^{2+}$  (circles) signal intensities on the concentration of sodium formate in BBY membranes obtained from the measurements shown in Figure 1a–d and for other concentrations. (b) A correlation between the loss of multiline (x-axis) signal intensity and the yield of formate-induced  $Q_A^-Fe^{2+}$  (y-axis) signal intensity obtained from (A). Approximate 10% errors are shown in each data curve.

trapped  $Y_Z^+$  radical signal was about 50% that of the  $Y_D^+$  signal, which was almost the same quantity as the decrease in the multiline intensity (Figure 1f). To confirm that the trapped signal could be assigned to the  $Y_Z^+$ , we carried out a “2 + 1” pulse sequence ESE experiment as described earlier (26, 27). The dark-adapted sample corresponding to trace 1 in Figure 3A shows no oscillatory behavior (Figure 3B (a)), which indicates there is only  $Y_D^+$  radical in PS II. On the other hand, an oscillating time profile of the primary echo signal is observed in the 253 K illuminated and trapped sample (Figure 3B (b)), which shows the dipole interaction between the trapped  $Y_D^+$  and  $Y_Z^+$  pair in the same reaction center.

**$O_2$  Evolution Measurements.** As an alternative test of formate inhibition, we measured the rate of oxygen evolution. In this experiment the membranes treated either with or without formate after centrifugation were resuspended in the same buffer as used for EPR. The results are illustrated in Figure 5, where low concentrations of less than 1 mM formate caused no appreciable changes in the rate of  $O_2$  evolution. The effective inhibition of oxygen-evolving activity induced by formate developed at formate concentrations of more than 5 mM. A drastic inhibition of oxygen-evolving activity started from 10 mM, and about 50% inhibition was accomplished at 40–50 mM formate treatment. Such drastic inhibition was continued until 100 mM formate treatment, which was followed by a gradual increase of inhibitory effect of up to 20% of the initial value at a range of formate over 100–500 mM. These results are in agreement with those

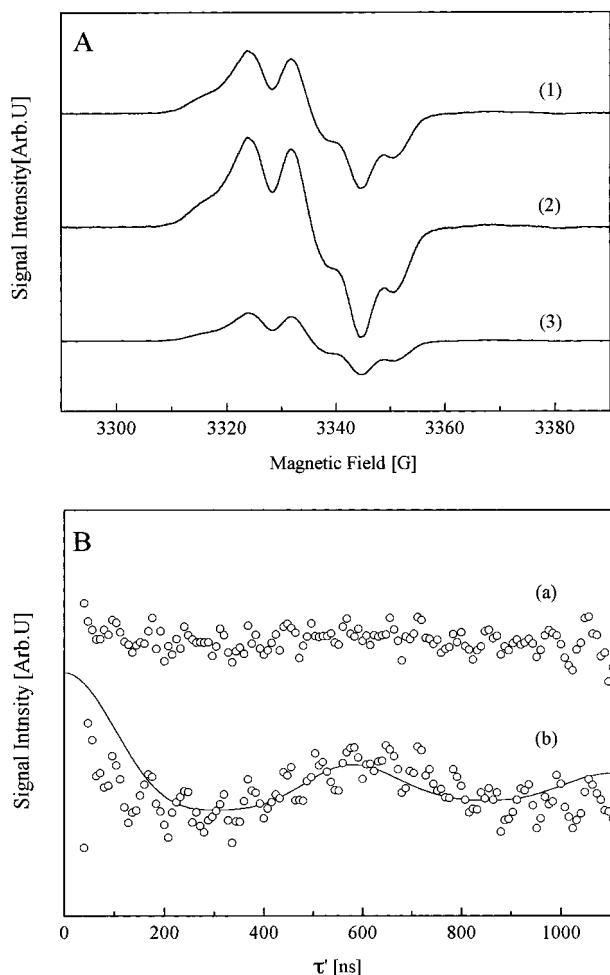


FIGURE 3: (A) Appearance of the  $Y_Z^+$  signal in the KM PS II particles with 250 mM formate concentration at pH 6.0 and without methanol (see the sample for Figure 1f) trapped in liquid  $N_2$ . Before (1) and after (2) illumination for 1 min at 253 K and the difference (3) = (2) - (1) that shows about 50% intensity of (1). Measurement conditions: microwave frequency 9.3 GHz, power 12.5  $\mu$ W, field modulation frequency 100 kHz, field modulation amplitude 3.2 G, temperature 77 K. (B) The  $Y_Z^+$  signal was identified by a "2 + 1" pulse sequence ESE. (a) The nonoscillating time profile indicates  $Y_D^+$  only in the dark-adapted PS II. After illumination and immediate trapping, the oscillating behavior indicates that there were two kinds of radical signals in the sample shown in part A (2). The curve is fitted with a simulation for the distance of 30 Å between the radicals that has been determined for  $Y_Z^+$  and  $Y_D^+$  radicals in ref 26. Measurement conditions: microwave frequency 9.61 GHz; the first 16 ns  $90^\circ$  and third 24 ns  $180^\circ$  spin rotation pulses with a separation of 1000 ns give a spin-echo signal; the second 24 ns  $180^\circ$  pulse produces dephasing of the spin-echo signal depending on the time of application  $\tau'$ , resulting in the oscillating time profile. The magnetic field was fixed at 3440 G corresponding to the lower field peak of the  $Y_D^+$  signal in part A (1).

observed with EPR both for inhibition in  $S_2$  state multiline formation and for evolution of the  $Q_A^-Fe^{2+}$  signal as described above. The values of the decrease in the multiline signal intensity and in the degree of inhibition in  $O_2$  evolution coincide only qualitatively, because the differences in the conditions of the measurements and illumination temperatures might have affected the degree of inhibition. In fact we observed no appreciable multiline and  $g = 4.1$  signals in the 90%  $Y_Z^+$ -trapped PS II caused during illumination (data not shown).

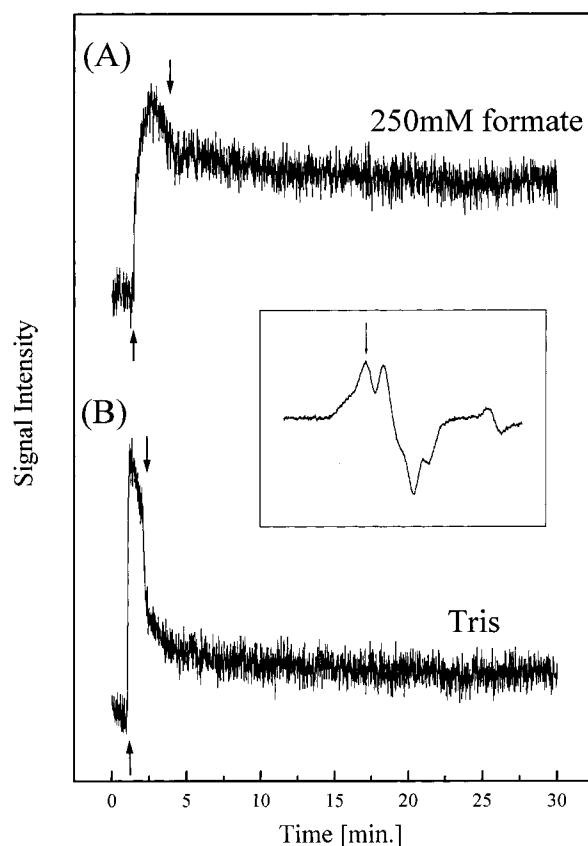


FIGURE 4:  $Y_Z^+$  signal kinetics observed in 253 K illuminated 250 mM formate-treated (A) and Tris-treated (B) KM PS II particles. The magnetic field was fixed at the lower field peak of the  $Y_D^+$  signal shown by an arrow in the inset. The arrows  $\uparrow$  and  $\downarrow$  show light on and off, respectively. EPR conditions are the same as in Figure 3A except for a microwave power of 0.8 mW and temperature of 253 K.

The inhibitory effect of formate on  $O_2$ -evolving activity was shown to be reversible. Almost complete restoration of  $O_2$  evolution activity of more than 90% of the value for a control sample was observed in formate-treated samples after being washed or resuspended with formate-free media. This indicates that even an extended treatment by formate did not cause any structural damage to the oxygen-evolving complex in PS II. Given these, the inhibitory effects may be due to a blockage in electron transport paths in PS II by specific binding of formate not only to the acceptor side but possibly also to the donor side.

**Fluorescence Characteristics.** Figure 6 shows the photo-induced changes of variable fluorescence  $F_V$  related to photoreduction of the  $Q_A$  electron acceptor at different concentrations of formate in the assay medium. The yield of fluorescence is believed to be proportional to the concentration of photochemically accumulated  $Q_A^-$  and is sensitive to the state of the PS II WOC. Here, low-intensity actinic light of 50  $W/m^2$  was used to measure the change of the yield and rise of  $F_V$ , revealing inhibition of the PS II donor side due to replacement of bicarbonate with formate anion. If we used saturated actinic light intensities, the electron transport in PS II would be limited by the photo-accumulation of the  $Q_A^-$  state, and quick establishment of a maximal level of fluorescence might take place before the measurement of  $F_V$ . As shown in curve 3 of Figure 6 the inhibition of variable fluorescence was not observed at a low

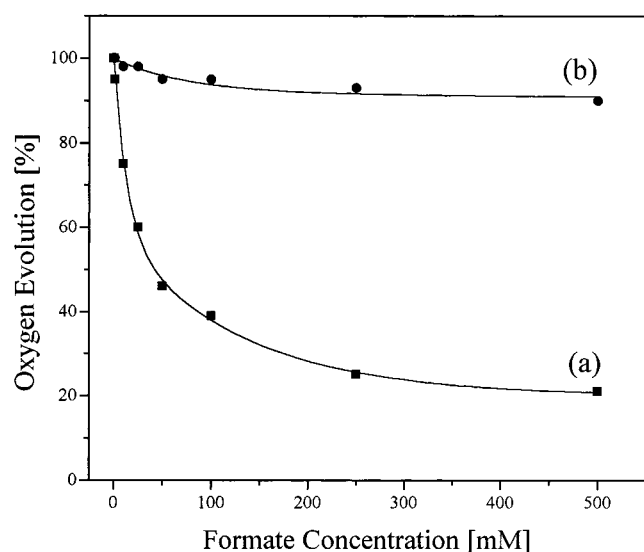


FIGURE 5: Dependence of oxygen-evolving activity on concentrations of sodium formate in BBY membranes: (a) membranes after formate treatment resuspended in the same medium with different concentrations of sodium formate and (b) membranes after treatment resuspended in the formate-less medium. An assay medium includes 50 mM MES–NaOH (pH 6.0), 300 mM sucrose, 5 mM NaCl, 5 mM  $\text{CaCl}_2$ , 1 mM EDTA, and 3% methanol. PPBQ (100  $\mu\text{M}$ ) was used as an electron acceptor. The rate of oxygen evolution of control samples was  $400 \pm 20 \mu\text{M O}_2 (\text{mg of Chl})^{-1} \text{ h}^{-1}$ .

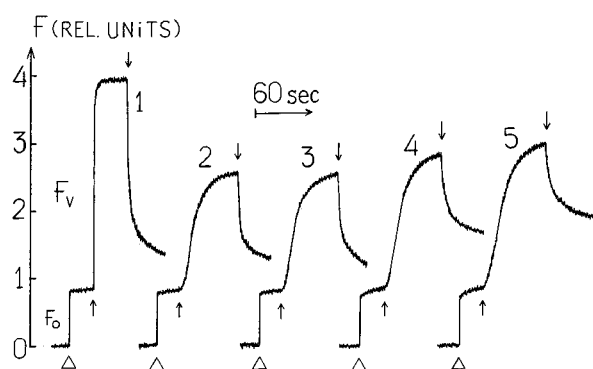


FIGURE 6: Effect of formate on the photoinduced changes of chlorophyll fluorescence related to  $\text{Q}_\text{A}$  photoreduction at actinic light intensities of 150  $\text{W/m}^2$  (1) and 50  $\text{W/m}^2$  (2–5): 1 and 2, for the control without addition of formate; 3–5, in the presence of formate at concentrations of 25  $\mu\text{M}$ , 25 mM, and 250 mM, respectively. Chlorophyll concentration: 10  $\mu\text{g/mL}$ . An assay medium consists of 50 mM MES–NaOH (pH 6.0), 35 mM NaCl, and 2 mM  $\text{MgCl}_2$ .  $\Delta$ , measuring light (0.05  $\text{W/m}^2$ ) on;  $\uparrow$  ( $\downarrow$ ), actinic light on (off).

concentration of formate (10–50  $\mu\text{M}$ ) in the assay medium in contrast with the results obtained in the digitonin-extracted membrane fragments (16, 17). However, the increase of  $F_\text{V}$  intensity took place upon the addition of formate at concentrations of more than 1 mM (curves 4 and 5). The extent of stimulation of chlorophyll fluorescence by formate was similar to the well-known effect of DCMU that inhibits electron transfer between  $\text{Q}_\text{A}$  and  $\text{Q}_\text{B}$  electron acceptors (43). In this experiment a slight increase in the chlorophyll fluorescence occurred for the  $F_0$  level with long-term measuring light in the presence of formate at concentrations of more than 25 mM, due to blockage of the electron transfer beyond  $\text{Q}_\text{A}$ . In this case, weak measuring light induced electron transfer in the RC, and therefore  $\text{Q}_\text{A}^-$  accumulated gradually. These data do not coincide with the EPR data nor

with the results on  $F_\text{V}$  in refs 16 and 17 that the low concentration of formate inhibited the donor side electron transfer.

## DISCUSSION

The importance of bicarbonate for oxygen-evolving activity was reported in the earlier studies (6, 7), and a model for water oxidation that takes bicarbonate into account as a mediator had been suggested (8). Later the acceptor side of PS II was shown to be responsible for bicarbonate binding (44). It is established that the binding site of formate is the non-heme iron located between  $\text{Q}_\text{A}$  and  $\text{Q}_\text{B}$ , and its inhibitory effect occurs in the competition with bicarbonate. It has been suggested that bicarbonate is one of the labile ligands to the non-heme iron (11–12, 15). The electron flow from  $\text{Q}_\text{A}^-$  to  $\text{Q}_\text{B}$  at normal velocities requires the binding of this anion to the non-heme iron.

In recent studies by Klimov et al. (16–20) the requirement of the bicarbonate for the donor side activity of PS II was suggested. They indicated that the inhibition of electron transport on the donor side requires much lower ( $1000^{-1}$  times) concentrations of formate than that on the acceptor side (16, 17) in the PS II membrane fragments used. The positive effect of bicarbonate was confirmed on recovery of electron transport by exogenous  $\text{Mn}^{2+}$  (16, 17), on protection of the donor side of PS II against photo- and thermoinactivation (45), and on the flash-induced changes in absorbance at the 295 nm, which relates to oxidation of manganese (18). It was suggested that bicarbonate probably took part in the formation of the functional Mn cluster or in regulation of its redox capacities as an essential ligand by itself or through modification of the binding site of Mn. Another investigation (46) has shown that the dark stable  $\text{S}_1$  state of the oxygen-evolving complex is modified by formate in the presence of sodium ascorbate and 2,6-dichloro-*p*-benzoquinone, which resulted in a high yield of the  $\text{S}_0$  state of PS II.

Thus, two alternative sites for formate and bicarbonate competition, which regulates the function of PS II, have been proposed by different groups, the non-heme iron of the acceptor complex (3–5, 11–15) and the donor side of PS II, probably at the Mn cluster (16–20). In the present study, the results are summarized as follows: (1) inhibition of the  $\text{S}_2$  state multiline signal formation and oxygen-evolving activity with formate; (2) evolution of the  $\text{Q}_\text{A}^- \text{Fe}^{2+}$  signal in the  $g = 1.82$  region; (3) absence of PS II inhibition at low concentrations of formate; (4) an appearance of the  $\text{Y}_\text{Z}^+$  radical; (5) a total restoration of the PS II activity after removal of formate. This might suggest that the bicarbonate binds more strongly to the putative binding site than the formate. It should be noted that (1) and (2) are well correlated with each other as shown in Figure 2B.

There may be two different views as follows to interpret the results obtained in this study.

(1) One possible explanation for the inhibitory effect by formate may be its interaction with the donor side components of PS II, presumably with the Mn cluster. This assumption was confirmed by the inhibition of the oxygen-evolving activity of PS II membranes and by the formation of the  $\text{Y}_\text{Z}^+$  radical induced by formate, which inhibited electron transfer from WOC to  $\text{Y}_\text{Z}^+$ . However, a rather high concentration of formate (10–100 mM) that is comparable



with formate concentration to inhibit the electron transfer between  $Q_A$  and  $Q_B$  was required for inhibition of the multiline signal formation. This concentration is different from that suggested in refs 16 and 17. We also could not find any effects of lower than 1 mM concentrations of formate on the variable fluorescence intensity and the rate of oxygen evolution. These disagreements might arise from the difference between membrane preparations used for the experiments. BBY particles were used in this study, whereas digitonin-extracted fragments of thylakoid membrane were used in refs 16 and 17. Oxygen-evolving activity of digitonin-extracted particles was reported to be  $120\text{--}150\ \mu\text{M O}_2\ (\text{mg of Chl})^{-1}\ \text{h}^{-1}$  (16), which shows that these particles consist of different sizes of polypeptides and probably include some defective oxygen evolving site. The inhibition of the PS II donor side occurred at rather high formate concentrations compared to that reported in refs 16 and 17. The result obtained in this work is similar to that in the acetate treatment, where a high concentration (hundreds of millimolar) of acetate was used for inhibition of the donor side reaction (25, 41, 42, 47). Formate binding affinity for the donor side seems to be comparable to that of the acceptor side in PS II. The difficulties in discrimination of the affinities on these two sides by spectroscopic methods probably originate from the similarity of the mode of binding to PS II from bicarbonate to formate. Since replacement of chloride by acetate has been suggested in previous works (25, 42, 47), a possibility for formate to replace chloride in PS II may be considered. It will be further necessary to determine whether the manganese cluster or  $Y_Z$  is responsible for formate binding.

We could not find any destructive effect of formate on the WOC in PS II. The  $\text{O}_2$ -evolving activity of the treated samples after depletion of formate was the same as that in control samples, which shows WOC had not been destroyed. The decrease in the  $S_2$  state multiline signal intensity might be due to some reversible structural changes induced by formate ligation during illumination or in the dark to a site close to the manganese cluster. The increase of the  $g = 4.1$  signal intensity (Figure 1c,d) with increasing formate concentration shows that formate may repel methanol coordinated to the site of the manganese cluster (48). Further increased formate might enter into the water coordination site, resulting in a decrease in the  $g = 4.1$  signal. The formate-induced  $g = 4.1$  signal produced in this way in PS II with 3% methanol was ascribed to an inactive site, suggesting that the inhibition was not totally derived from the replacement of the methanol-coordinated site.

(2) Alternatively, formate-induced inhibition of the multiline signal and oxygen-evolving activity of PS II membranes is ascribed to the interaction of formate to the acceptor side of PS II. The redox state of the  $Q_A\text{--Fe}^{2+}$  complex may be important for the S state configurations of PS II, and the changes in the structural properties of this complex may affect the stability of the S states. The results in this work show that the enhancement of the  $Q_A\text{--Fe}^{2+}$  signal is well correlated with the inhibition of the multiline signal. The linear relation between the increase in the formate-induced  $Q_A\text{--Fe}^{2+}$  and decrease in the multiline signal intensities suggests that the formate inhibition on the donor side may be induced by the inhibition at the acceptor side. On the other hand, it is not neglected that the binding constants

happen to be almost the same for the donor and acceptor sides, resulting in a linear relation. Therefore, the results obtained here from EPR measurements may give rise to a controversy that the inhibition of the  $S_2$  state multiline signal formation and oxygen-evolving activity was caused by the binding of formate to either the PS II donor side or the PS II acceptor side. The dependence of the inhibition of the  $S_2$  state multiline signal on the acceptor side agrees with the investigation (49) in newly prepared D1 mutants of *Chlamydomonas reinhardtii*, in which the site-directed mutagenesis of arginine 257 in the D1 polypeptide into glutamate (D1-R257E mutant) or methionine (DQ-R257M mutant) was engineered. Kinetic fluorescence studies of these mutants have shown a reduced sensitivity to formate as well as a significantly reduced rate of oxygen evolution. This finding shows the responsibility of the PS II acceptor side for formate and bicarbonate effects in the above-mentioned mutants. The detailed mechanisms of regulation of the donor side by the acceptor side remain to be studied.

The results obtained in this study have suggested that formate inhibits the donor side reaction of PS II by slowing electron transfer on the donor side of PS II through a weak binding to some site in the WOC. This is confirmed by the absence of any destructive effect by formate and total restoration of activity of the PS II donor side from the inhibition induced by formate. The appearance of the  $Y_Z^+$  signal indicates that the electron transfer from the Mn cluster to  $Y_Z^+$  has been retarded. The conversion of the  $S_2$  state multiline signal to the  $g = 4.1$  signal in the presence of formate suggests that the electron transfer to  $Y_Z^+$  is slowed possibly in the  $S_2$  state of the WOC. However, it is still unclear whether the inhibitory effect of formate in the PS II donor side is a consequence of the regulation by the acceptor side due to its binding with formate or merely due to a direct effect of formate on the donor side of PS II. These two possibilities are to be discriminated by further studies.

## ACKNOWLEDGMENT

We thank Dr. Andrei V. Astashkin and Dr. Hiroyuki Mino for critical discussions on this work. We are indebted to Mr. M. Tonaka in this laboratory for ESE measurements.

## REFERENCES

1. Debus, R. J. (1992) *Biochim. Biophys. Acta* 1102, 269–352.
2. Diner B. A., and Babcock G. T. (1996) in *Oxygenic Photosynthesis: The Light Reactions* (Ort, D. R., and Yocum, C. F., Eds.) pp 213–247, Kluwer Academic Publishers, Dordrecht, The Netherlands.
3. Govindjee, and Van Rensen J. J. S. (1978) *Biochim. Biophys. Acta* 505, 183–213.
4. Govindjee, and Van Rensen, J. J. S. (1993) in *In the Photosynthetic Reaction Center* (Deisenhofer, J., and Norris, J. R., Eds) Vol. 1, pp 357–389.
5. Van Rensen, J. J. S., Xu C., and Govindjee (1999) *Physiol. Plant.* 105, 585–592.
6. Stemler, A., and Govindjee (1973) *Plant Physiol.* 52, 119–123.
7. Stemler, A., Babcock G. T., and Govindjee (1974) *Proc. Natl. Acad. Sci. U.S.A.* 71, 4679–4683.
8. Jursinic, P., Warden, J., and Govindjee (1976) *Biochim. Biophys. Acta* 440, 322–330.
9. Stemler, A. (1977) *Biochim. Biophys. Acta* 460, 511–522.
10. Stemler, A. (1980) *Biochim. Biophys. Acta* 593, 103–112.
11. Petrouleas, V., and Diner, B. A. (1990) *Biochim. Biophys. Acta* 1015, 131–140.

12. Diner, B. A., and Petrouleas, V. (1990) *Biochim. Biophys. Acta* 1015, 141–149.
13. Deligiannakis, Y., Petrouleas, V., and Diner, B. A. (1994) *Biochim. Biophys. Acta* 1188, 260–270.
14. Petrouleas, V., Deligiannakis, Y., and Diner, B. A. (1994) *Biochim. Biophys. Acta* 1188, 271–277.
15. Hienerwadel, R., and Berthomieu, C. (1995) *Biochemistry* 34, 16288–16297.
16. Klimov, V. V., Allakhverdiev, S. I., Feyziev, Ya. M., and Baranov, S. V. (1995) *FEBS Lett.* 363, 251–255.
17. Klimov, V. V., Allakhverdiev, S. I., Baranov, S. V., and Feyziev, Ya. M. (1995) *Photosynth. Res.* 46, 219–225.
18. Vincencjusz, H., Allakhverdiev, S. I., Klimov, V. V., and Van Gorkom, H. J. (1996) *Biochim. Biophys. Acta* 1273, 1–3.
19. Allakhverdiev, S. I., Yruela, I., Picorel, R., and Klimov, V. V. (1997) *Proc. Natl. Acad. Sci. U.S.A.* 94, 5050–5054.
20. Klimov, V. V., Hulsebosch R. J., Allakhverdiev, S. I., et al. (1997) *Biochemistry* 36, 16277–16281.
21. Berthold, D. A., Babcock, G. T., and Yocum, C. F. (1981) *FEBS Lett.* 134, 231–234.
22. Ghanotakis, D. F., Topper, J. N., and Yocum, C. F. (1984) *Biochim. Biophys. Acta* 767, 524–531.
23. Arnon D. I. (1949) *Plant Physiol.* 24, 1–15.
24. Kuwabara, T., and Murata, N. (1982) *Plant Cell Physiol.* 23, 533–599.
25. MacLachlan, D. J., and Nugent, J. H. A. (1993) *Biochemistry* 32, 9772–9780.
26. Astashkin, A. V., Kodera, Y., and Kawamori, A. (1994) *Biochim. Biophys. Acta* 1187, 89–93.
27. Kodera, Y., Hara, H., Astashkin, A. V., and Kawamori, A. (1995) *Biochim. Biophys. Acta* 1232, 43–51.
28. Dismukes, G. C., and Siderer, Y. (1981) *Proc. Natl. Acad. Sci. U.S.A.* 78, 274–278.
29. Casey, J. L., and Sauer, K. (1984) *Biochim. Biophys. Acta* 767, 21–28.
30. Zimmermann, J.-L., and Rutherford, A. W. (1984) *Biochim. Biophys. Acta* 767, 160–167.
31. Zimmermann, J.-L., and Rutherford, A. W. (1986) *Biochemistry* 25, 4609–4615.
32. De Paula, J. C., Innes, J. B., and Brudvig, G. B. (1985) *Biochemistry* 24, 8114–8120.
33. Hansson, O., Aasa, R., and Wanngard, T. (1987) *Biophys. J.* 51, 825–832.
34. Pace, R. J., Smith, P., Bramley, R., and Shetlik, D. (1991) *Biochim. Biophys. Acta* 1058, 161–170.
35. Britt, R. D., Lorgian, G. A., Sauer, K., Klein, M. P., and Zimmermann, J. L. (1992) *Biochim. Biophys. Acta* 1140, 95–101.
36. Haddy, A., Dunham, W. H., Sands, R. H., and Aasa, R. (1992) *Biochim. Biophys. Acta* 1099, 25–34.
37. Astashkin, A. V., Kodera, Y., and Kawamori, A. (1994) *J. Magn. Reson. (Ser. B)* 105, 113–119.
38. Miller, A.-F., Brudvig, G. W. (1992) *Biochim. Biophys. Acta* 1056, 1–18.
39. Vermaas, W. F. J., and Rutherford, A. W. (1984) *FEBS Lett.* 175, 243–248.
40. Shigemori, K., Mino, H., and Kawamori, A. (1997) *Plant Cell Physiol.* 38, 1007–1011.
41. Szalai, V. A., and Brudvig, G. W. (1996) *Biochemistry* 35, 1946–1953.
42. Force, D. A., Randall, D. W., and Britt, R. D. (1997) *Biochemistry* 36, 12062–12070.
43. Velthuys, B. R. (1981) *FEBS Lett.* 126, 277–281.
44. Wydrzynski, T., and Govindjee (1975) *Biochim. Biophys. Acta* 387, 403–408.
45. Klimov, V. V., Baranov, S. V., and Allakhverdiev, S. I. (1997) *FEBS Lett.* 418, 243–246.
46. Stemler, A. J., and Lavergne, J. (1997) *Photosynth. Res.* 51, 83–92.
47. Kühne, H., Szalai, V. A., and Brudvig, G. W. (1999) *Biochemistry* 38, 6604–6613.
48. Force, D. A., Randal, D. W., Lorigan, G. A., and Britt R. D. (1998) *J. Am. Chem. Soc.* 120, 13321–13333.
49. Xiong, J., Minagawa, J., Crofts, A., and Govindjee (1998) *Biochim. Biophys. Acta* 1365, 473–491.

BI992479H